

# We are IntechOpen, the world's leading publisher of Open Access books Built by scientists, for scientists

5,300

Open access books available

130,000

International authors and editors

155M

Downloads

Our authors are among the

154

Countries delivered to

TOP 1%

most cited scientists

12.2%

Contributors from top 500 universities



WEB OF SCIENCE™

Selection of our books indexed in the Book Citation Index  
in Web of Science™ Core Collection (BKCI)

Interested in publishing with us?  
Contact [book.department@intechopen.com](mailto:book.department@intechopen.com)

Numbers displayed above are based on latest data collected.  
For more information visit [www.intechopen.com](http://www.intechopen.com)



# Laser Surface Modification of Materials

*Natarajan Jeyapraakash, Che-Hua Yang  
and Durairaj Raj Kumar*

## Abstract

The metallic materials such as steel, iron, titanium and nickel alloys etc., are extensively used in the automobile, marine, biomedical, aerospace, chemical industry and power generation sector. However, the poor surface properties restricted their wide usage in many applications. Therefore, the surface properties need to be enhanced through novel treatments without affecting the bulk. In recent years, laser surface modification attracts more due to their inherent properties. The laser based surface altering process is appropriate to modify the metallic surfaces in terms of their flexibility, simple operation and process economy. Laser surface modification includes; surface hardening, melting, alloying, cladding and texturing. Thus, from a process engineering, metallurgical reasons and tribologist view point, the laser surface modification process can be recognized as an important topic.

**Keywords:** laser hardening, melting, alloying, cladding and texturing

## 1. Introduction

In the 20th century, Laser surface alteration played a major role in enhancing the material surface properties. Among the number of ways to enhance the material properties, laser based surface alterations are used to enhance a better physical property in the machined surface and improved the component performance. The high power Neodymium Yttrium-Aluminum-Garnet (Nd: YAG) laser, carbon-dioxide (CO<sub>2</sub>) laser and excimer lasers are used to perform the laser surface treatment which is expensive, popular and operate at pulsed mode or continuous wave mode. These lasers are used to heat the near-surface area of the finished components for enhancing the properties. The laser surface modifications have the ability to control the amount of heat energy to work material with high directionality. The purpose of a surface hardening by laser is to improve the component wear properties. The laser surface hardening is defined as the heat energy from the laser beam that directly heated the component surface at a very short interval period without melting the work material. The heat input to the component surface is the reason for creating the tough and fine-grained structure in the hardened surface. The risk of crack forming is very low due to the self-quenching process. The laser surface melting (LSM) is heated to its melting point through a high power laser beam and rapidly solidified. The aim of LSM is to refine the surface microstructure, homogenization of composition, dissolution of precipitates. The LSM is also used to improve the corrosion resistance of steel and iron. The minimization of intergranular corrosion

is possible through LSM by avoiding the carbides formation during subsequent homogenization and sensitizing treatment. The laser surface alloying (LSA) is defined as the high heat energy used to melt the metal coating through laser and a portion of underlying substrate. This technique is used to form highly resistant gradient layers on the metal surface. The major benefit of this technique is sudden heating followed by cooling and the surface properties are improved. The laser cladding (LC) is a coating method that the surface melting and new material layer formation by addition of material are simultaneously processed in the substrate at the same time by using the laser power. The desired surface properties are achieved after solidification. The large component surface properties are easily increased by using LC. The complete metallurgical bond is necessary between the melting of substrate and forming of a new material layer at the interface. The laser surface texturing (LST) is defined as the process in which the change of material surface properties by modifying its texture and roughness. The laser beam is used to create the micro patterns on the surface by laser ablation. The micro patterns are created on the surface in various shapes such as dimples, grooves and free forms with precise dimension. This process is mostly used in biomedical applications.

The different types of laser have different abilities to perform the process on materials. All the lasers are producing the heat energy and the laser beam wavelength is majorly affecting the performance of materials. Generally, the total laser heat energy is supplied to work material in which can be divided into two ways such as the fraction of heat energy is observed by work material and remaining heat energy is reflected to the environment. This happens during the surface hardening by laser. The supply of heat energy to polished metal surface components is depending upon the heat absorbability of work material and wavelength of irradiation. Generally, the short wavelength has higher absorptivity. Hence, the Nd: YAG laser ( $\lambda = 1.064 \mu\text{m}$ ) has produced the higher absorbing ability beam to work material than the CO<sub>2</sub> laser ( $\lambda = 10.6 \mu\text{m}$ ) for surface hardening of steel. In order to increase the CO<sub>2</sub> laser absorbability (high wavelength) to work material, the coating or painting is required in the work material prior to the CO<sub>2</sub> laser surface hardening. Therefore, the Nd: YAG laser surface hardening better than CO<sub>2</sub> laser surface hardening because the Nd: YAG laser has short wavelength and produces a high absorbing rate to work material. The Nd: YAG laser produces heat energy to work material which is transferred through fiber cable whereas CO<sub>2</sub> laser is impossible. The inert gases, helium, neon and argon are used to eliminate the atmospheric contamination. In order to reduce the wavelength of a laser, an excimer laser is developed with very short wavelength. This laser can be used to micromachining on medical parts. In this chapter, laser surface hardening, laser surface melting, laser surface alloying, laser surface cladding and laser surface texturing have been discussed to improve the microstructure, hardness and wear resistance of mechanical components.

## **2. Laser surface hardening (LSH)**

The laser surface hardening is defined as the heat energy from the laser beam which is directly impacted to the finished component surface for improving the wear resistance. The component life is increases without affecting the bulk material. During the hardening process, the surface layer is heated up to hardening temperature under the short period of time. The quenching is a necessary process to achieve the hard martensite phase in the heated surface. Thereby, the component surfaces are hardened by laser and achieve the high wear resistant surface with desired bulk properties. The components such as gear teeth, gears, shafts, camshafts, axles, cylinder liners, valve guides and exhaust valves showed with higher

stresses due to laser surface hardening. The type of work materials, cast iron, die steel and medium-carbon steel are also required the laser surface hardening for better performance. The mass-production industries, automobile components and electronic parts are performed the laser hardening on the component surfaces [1]. The desired component performances are mainly depending upon the selection of laser process parameters such as power, scanning speed, pressure, beam shape and material properties. Now-a-days, in order to improve the surface quality of components, the number of surface treatment are commercially available to obtain the unique material properties. For example, the I-section rail (railway) is fabricated by hot rolled processes which have non-uniform properties in the flange and web. The I-section beam is shown in **Figure 1**. The flanges have been designed to withstand high stress whereas the web designed to withstand the least stress. The flange thickness is greater than the web thickness and stress developed in the I-section is within the allowable limit. The point is the different cross section of flange and web has produced the non-uniform properties. Hence, the laser surface hardening is required for achieving the uniform properties over the flange and web.

The laser surface transformation hardening process is performed to obtain the required depth and width for steel material. The accurate parts are made of medium carbon steels which require the laser surface hardening. The small and complex components are easily surface hardened by laser. This is because of the high rate of cooling effects to increase the hardness rate in the quenching process [2]. Therefore, LSH is a better process compared to flame and induction hardening processes. The quenching process is suddenly reducing the work material temperature by using water, oil or air to get certain material properties through the phase transformation. Therefore, a comparative study is made between the laser quenching and conventional quenching on steel to study the hardness and wear rate. The conventional quenching and tempering is carried out by using the temperature of 1198 K for 4.5 h and temperature of 523 K for 4 h respectively. The air, 10 kW CW diode laser, 3.5 mm spot diameter and 168 mm/s linear speed are used in the laser treatment. The laser quenched and conventional quenched sample for 25  $\mu\text{m}$  distance from the surface, the produced hardness is 600  $\text{HV}_{0.1}$  and 625  $\text{HV}_{0.1}$  respectively. The laser quenched sample has 0.4  $\text{mm}^3/\text{N-m}$  wear rate which is lesser than the conventional quenched sample of 0.6  $\text{mm}^3/\text{N-m}$  wear rate at 500 m sliding distance [3]. The wear and microhardness studies are performed on 40CrNiMoA steel by using laser quenching and high-frequency quenching.

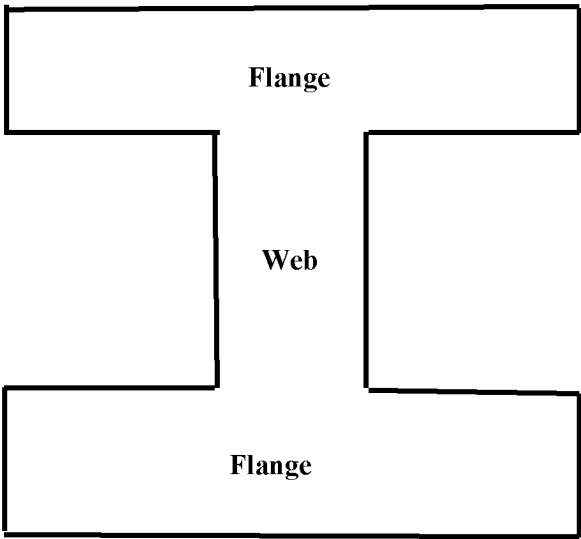


**Figure 1.**  
*Schematic of I-section beam used in rail.*

A 2 kW CW CO<sub>2</sub> laser, 1400 W laser power, 35 mm/s traverse speed, 60 degree incident angle, black organic absorbent coating, 0.9 m<sup>3</sup>/h gas flow rate and 10 mm defocusing distance are used in the laser treatment. The hardness of the quenched groove surface reached 750 HV and is substantially higher than that resulting from the high-frequency quenching method. The results of wear testing showed that the wear resistance of laser quenched specimens is 1.3 times higher than that of a high-frequency quenching specimen [4]. Comparisons were made between the gray cast iron (GCI), laser hardened quench-tempered GCI and conventional austempered GCI specimens based on the hardness and wear loss. The air, CW Nd: YAG laser, 2 mm laser spot, 22 mm defocused distance, 2 mm/s scanning speed, 6 Hz frequency, 120 A current and 8 ms pulse duration is used for laser hardening. The hardness of the laser hardened zone with ledeburitic structure is approximately 68 HRC. The quenching-tempered GCI specimen showed higher wear resistance than untreated GCI specimen [5].

The advantage of laser surface hardening is listed below

- The lower level of heat energy is used to work material compared to conventional surface heat treatment.
- The input laser energy is controlled by varying the process parameters such as power, scanning speed, defocus, different shapes of lenses and mirrors.
- The hardened surface is obtained through self-quenching of the heated surface layer.
- The work material is made under the hardening and quenching process resulting in cleaning of work material is not required.
- The beam guidance is automatically controlled over the work material.
- The surface heat treatment is specifically performed on small parts and complex parts.

The disadvantage of laser surface hardening is listed below

- High initial capital cost
- Skilled operators are needed
- Surface preparations are required in difficult areas.
- Radiation protection is required
- Material hardness and wear

The performance of the components such as hardness and wear resistance of work materials are mainly focused in the laser surface hardening. This is depending upon the material type, material properties, and types of processing on materials. The desired properties of work materials are obtained through proper selection of laser surface treatment and optimization. In order to improve the durability of mechanical components namely gears, engine valve, brake drums and camshaft are highly needed the LSH. The induction hardening is one of the surface hardening process which is shown in **Figure 2**. It is performed to achieve the uniform



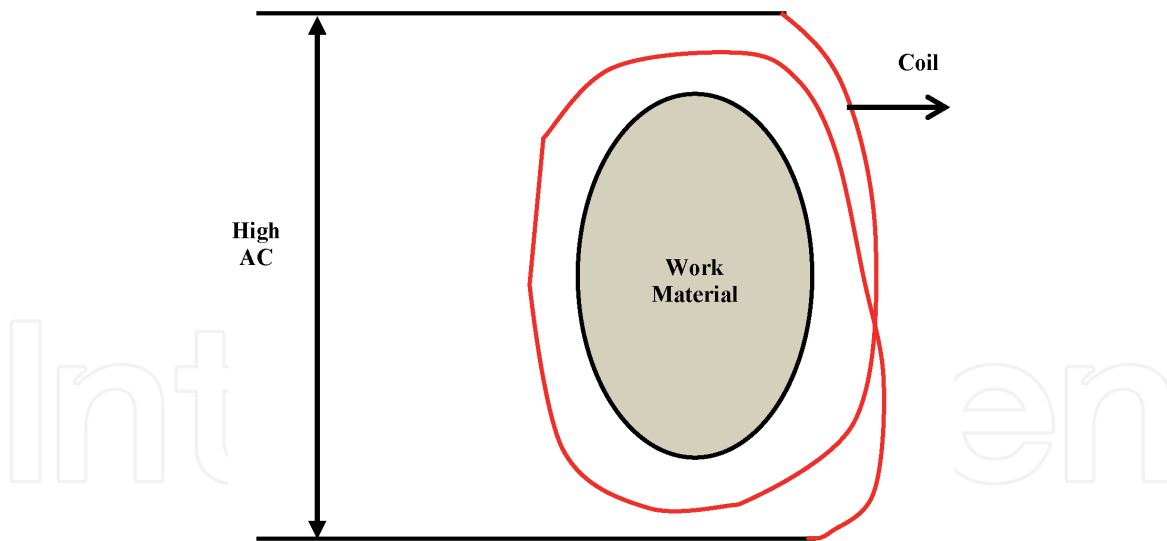


**Figure 2.**  
*Schematic of induction hardening.*

microstructure and good wear resistance which is higher implementation cost compared to laser surface hardening.

In this induction hardening, the depth of hardening is mainly depending upon the resistivity ( $\rho$ ), frequency ( $\nu$ ) and magnetic permeability ( $\mu$ ). The work material is placed inside the coil and supplies the high frequency. The surface is hardened by skin effect.

$$d = \sqrt{\frac{\rho}{\mu \nu}} \quad (1)$$

The laser surface hardening can be performed on the components either partially or fully depending upon the application of the components. Specifically, the load bearing component is subjected to high surface wear. Hence, the laser surface hardening is required on the load bearing component surface. Therefore, the load bearing component is hardened by laser, the surface has produced a high hardenability and fine microstructure [6]. The service life of crankshaft and camshaft are made on EN18 steel in which properties are improved by diode laser surface hardening with beam diameter of 3 mm, velocity of 1 m/min and power of 1.5 kW. The argon gas is used as shield gas [7]. The advantages of induction hardening are localized areas heat treated, minimal surface decarburization, surface oxidation, slight deformation, improved fatigue strength and low operating cost. The disadvantages of induction hardening are high capital investment. The advantages of laser hardening are described as non-hardenable steels are surface hardened, higher hardness obtained than conventional hardening, eliminating dimensional distortion, no protective atmosphere required and very long and irregular shapes easily hardened. The disadvantages of laser hardening are high initial and working cost and difficult to harden the high alloy steel. The schematic diagram of substrate and laser processed materials are shown in **Figure 3(a)** and **(b)**. The parent substrate has coarse and uneven equiaxed grains. The laser processed work material showed the hardened depth varying from top surface to 200  $\mu\text{m}$  depth. The depth of hardening increases with grain size increases from finer to coarser. The curved surface is formed at top surface due to the low scanning speed produces more evaporation in the laser melted surface. The laser process parameters, power of 1.5 kW, beam diameter of 3 mm, scan speed of 1 m/min and interaction time of 0.18 s are used to obtain the desired hardness. The Nd: YAG laser and argon gas with flow rate of 20 L/min is used in the laser surface hardening. The hardness decreases from 955 HV to

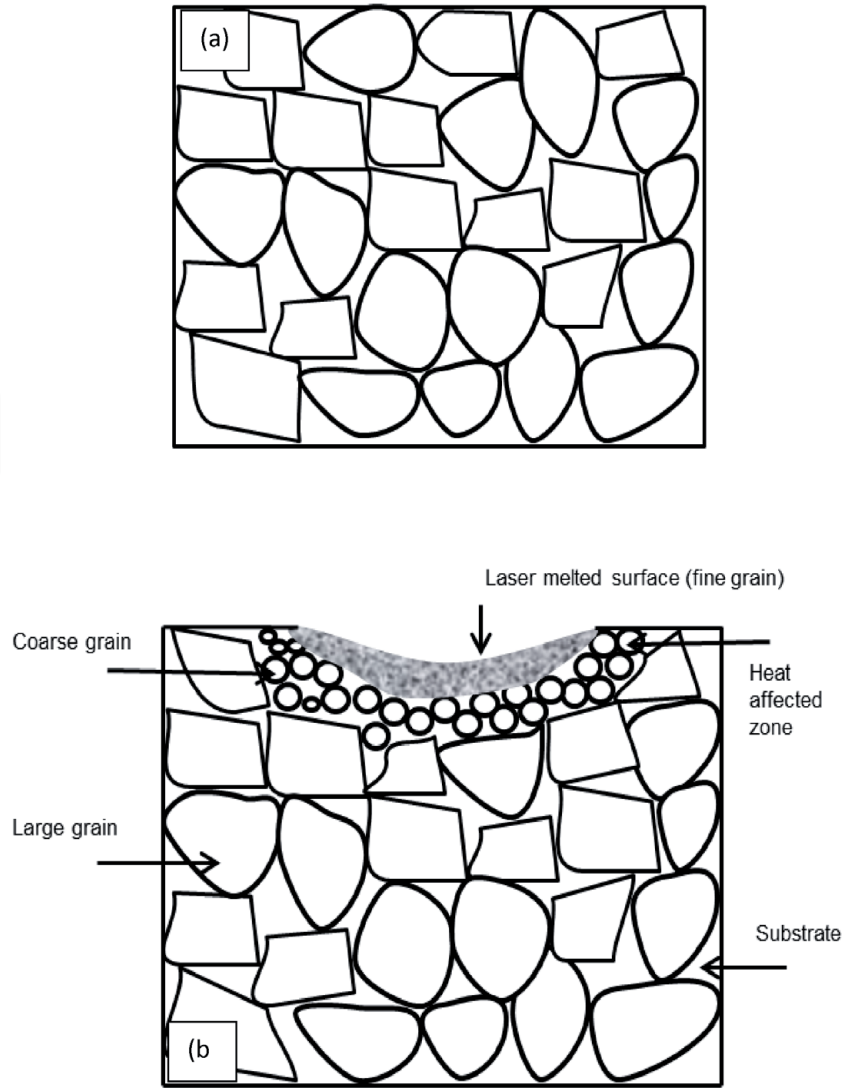


**Figure 3.**  
 (a) Schematic of; (a) as received tool steel microstructure, (b) laser surface hardened tool steel with modified structure.

236 HV which is obtained by varying distance from top to 200-micron depth and it is shown in **Figure 4**. This is due to the grain size refinement [8]. The 5 kW CW CO<sub>2</sub> laser, power ranging from 1.1–2.5 kW, traverse speed ranging from 6 to 15 mm/s and spot size of 6.3 mm, 2.27 mm, 4.63 mm and 1.2 mm are used to harden the various carbon steel. The argon gas is used as shielding gas. The traverse speed has mostly affecting the hardness. The carbon percentage increases, the average hardness value also increases. The C-45 steel has produced higher hardness. The hardness of the material was improved by minimizing the diameter of spot size [9]. Further, conventional type laser surface treatment is performed on large surface areas and irregular hardness was observed on the machined component. In order to overcome irregular hardness, a laser overlapping method is used in the laser transformation hardening which is presented in **Figure 5**.

After the laser treatment, the laser hardened zones are divided into three sections such as hardened zone, transition zone and heat affected zone which is shown in **Figure 6**. A study on the effect of process parameters on surface hardness splined shafts is performed by using laser surface hardening. The fiber laser, power varying from 1900 to 2500 W, scanning speed varying from 2 to 6 mm/s, rotation speed varying from 1500 to 2500 rpm, the flank tilt angle of spline tooth varying from 15 to 20 and tooth depth of spline shaft varying from 2.5–3.5 are used in the laser

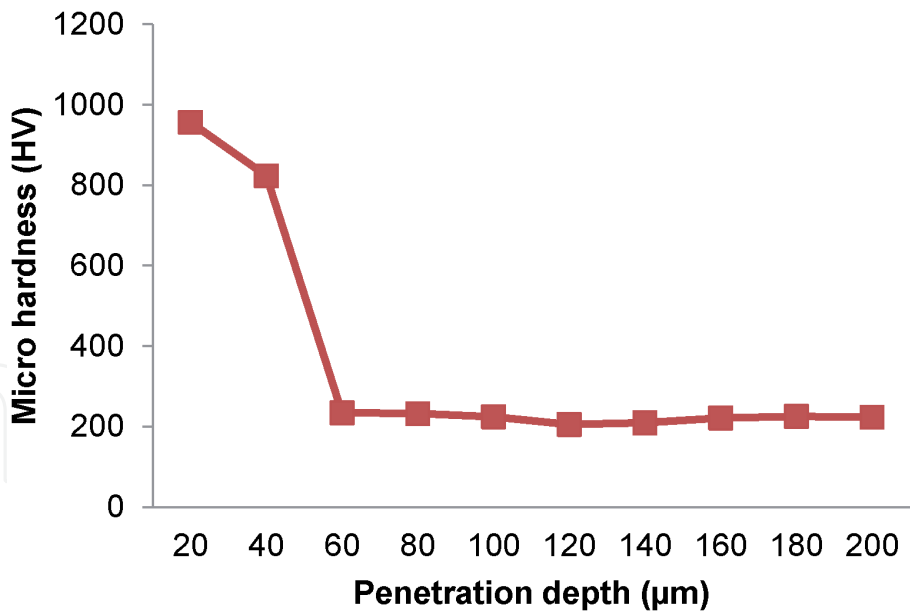


**Figure 4.**  
*Microhardness variation from top surface to substrate through LSH.*

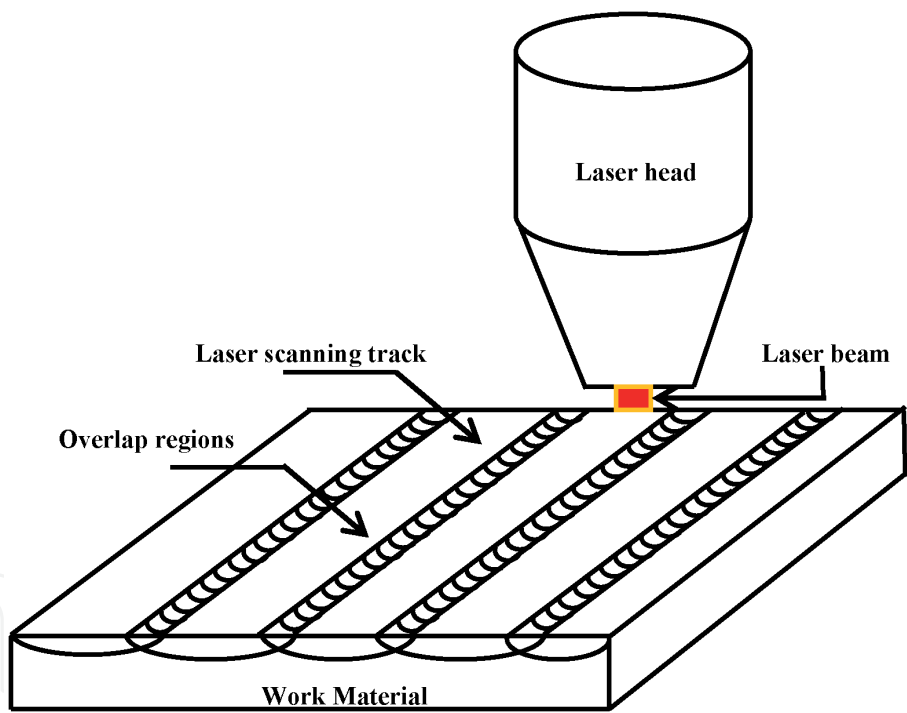


**Figure 5.**  
*Schematic of laser transformation hardening.*

hardening of spline shaft. The result found that the maximum hardness is observed by using the power of 2500 W, scanning speed of 2 mm/s, rotational speed of 2500 rpm, the flank tilt angle of spline tooth of 20° and tooth depth of spline shaft of 3.5 mm [10]. An investigation on the underwater hardening of AISI 1055 steel is carried out using lasers. A 250 W CW Ytterbium based fiber laser, focal length of 300 mm, defocus distance of 10 mm and traverse speed varying from 1 to 100 mm/s are used in the laser surface hardening. The result found that the higher surface roughness is obtained in the underwater welding compared to conventional laser hardening due to the additional cooling effect in the underwater [11].



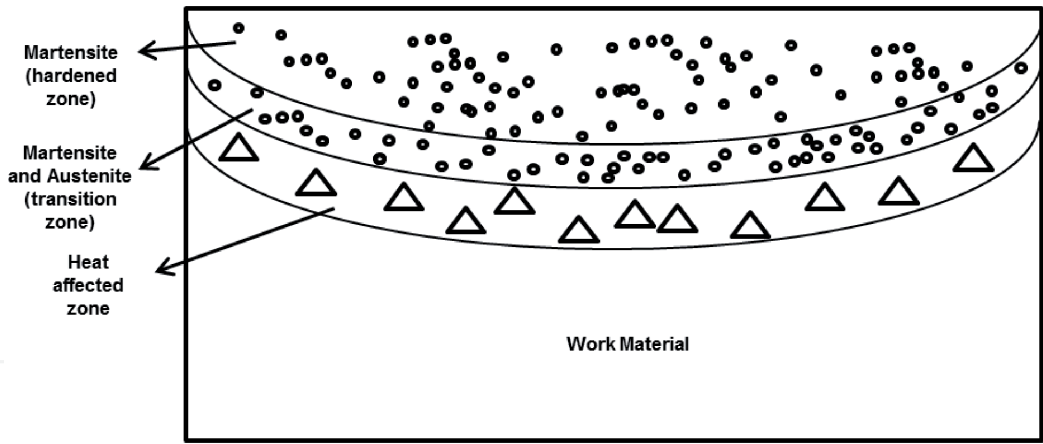


**Figure 6.**  
*Schematic of different zones of laser transformation hardening.*

**3. Laser surface melting (LSM)**

Laser surface melting is one of the surface alteration processes that the surface of the substrate is melted and rapidly solidified to form the fine microstructure and improving the mechanical properties without changing the bulk properties and without addition of any metallic elements. The piston, valve and sliding parts are made of magnesium alloys, which are used in the automobile components and energy saving material. The application and limitation of magnesium alloy is decided by properties. In order to improve the tribological and mechanical properties, the laser surface melting process is focused on magnesium alloy. In the conventional heat treatment of HSS materials are presented the retained austenite, which transforms into brittle martensite during service. But, the life of high-speed tool steel is increased by using LSM. The schematic view of LSM is shown in **Figure 7**. The LSM treatment are carried out using a 2 kW fiber laser with 1.06  $\mu\text{m}$  wavelength, laser power of 1500 W, the laser scanning speed of 600 mm/min and the distance between the laser head, spot size of 3 mm, shielding gas pressure of 0.3 MPa and the specimen

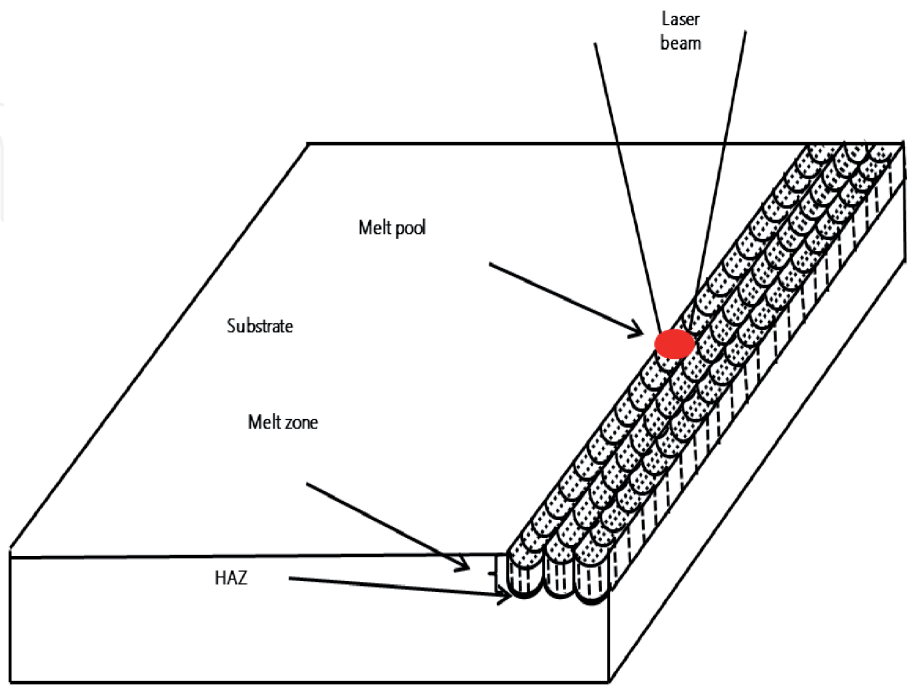


**Figure 7.**  
*Schematic view of laser surface melting.*

surface of 12 cm are used in the LSM. The microhardness and corrosion resistance of magnesium alloy is also improved by using LSM with electromagnetic stirring [12]. In order to enhance the microhardness of melted substrate, the LSM process parameters effect of hardness of magnesium alloy is studied. The CW CO<sub>2</sub> laser, beam diameter of 4 mm, argon gas of 6 l/min, speed varying from 100 to 400 mm/min and power varying from 1.5–3.0 kW are used in the process. The result showed that the melt depth of magnesium alloy is directly proportional to the laser power and inversely proportional to the scan speed. Laser surface melting enhances the microhardness of the melted zone by 2–3 times than the substrate [13]. The laser processed hardness of high speed tool steel and magnesium alloy is decreased from as-received substrate by increasing distance from the melting surface which is shown in **Figure 8**. This is due to the refined, solid solution strengthening and uniform microstructure. The LSM is also performed in electric contact material of Cu-50Cr. The 1 kW CW Nd: YAG laser, power density varying from 10<sup>6</sup> to 10<sup>7</sup> W/cm<sup>2</sup>, scanning speed of 6000–10,000 mm/min and argon gas are used in this process. From the analysis found that the microhardness and withstanding voltage of Cu-50Cr are significantly improved by using LSM [14]. The effects of LSM process parameters are affecting the microstructure and hardness of AZ31B magnesium alloy substrate. The result found that the grain size in the fused layer increases by increasing power. The schematic diagram of as-received magnesium alloy is shown in **Figure 9a**. The effects of different power on microstructure of layer fused layers are shown in **Figure 10 b-e**. The Nd: YAG laser power varying from 1600 to 2200 W, laser beam scanning velocity of 900 mm/min, laser beam spot diameter of 4 mm, number of superimposed tracks of 9, overlap ratio of 15%, and argon flow rate of 25 mL/min are used in the process. The depth of the metal pool and grain size is increased by increasing the power. This is due to the grain growing freely in the higher metal pool depth compared to smaller metal pool depth. The reason for increasing the hardness and wear resistance are

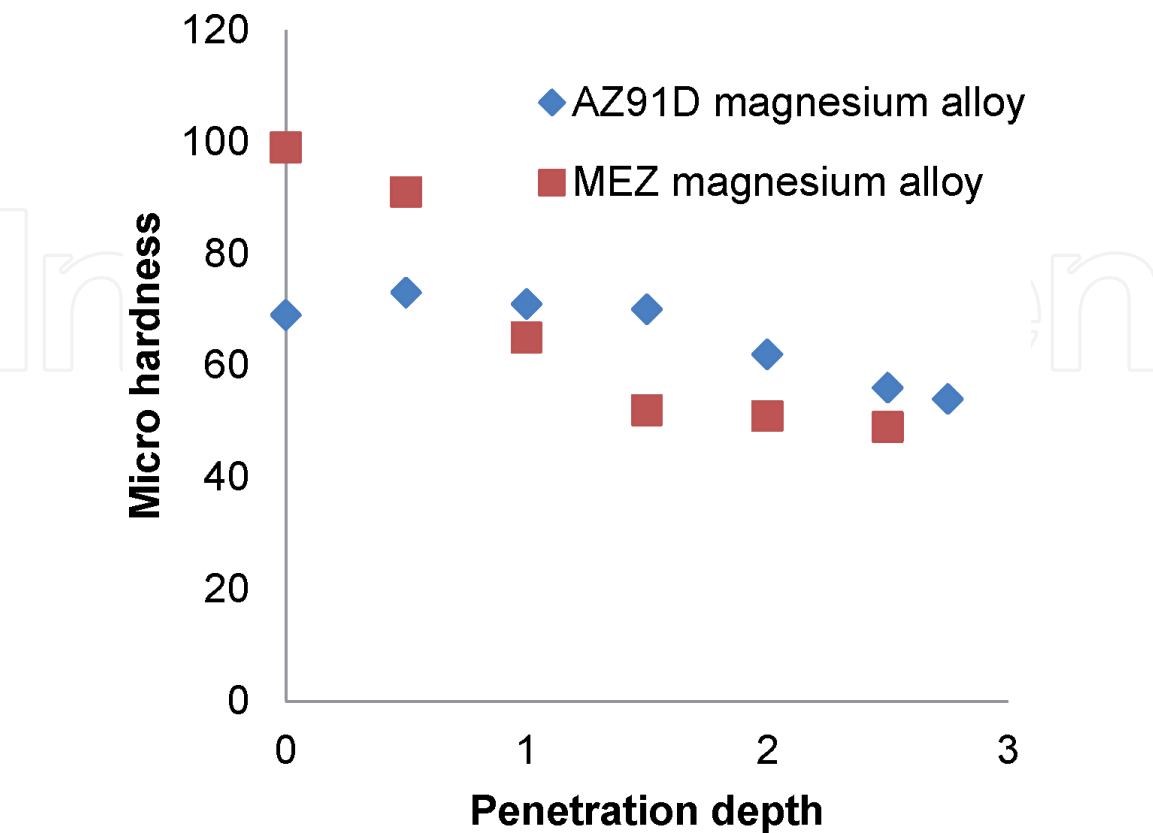


**Figure 8.**  
*Microhardness variation of magnesium alloy.*

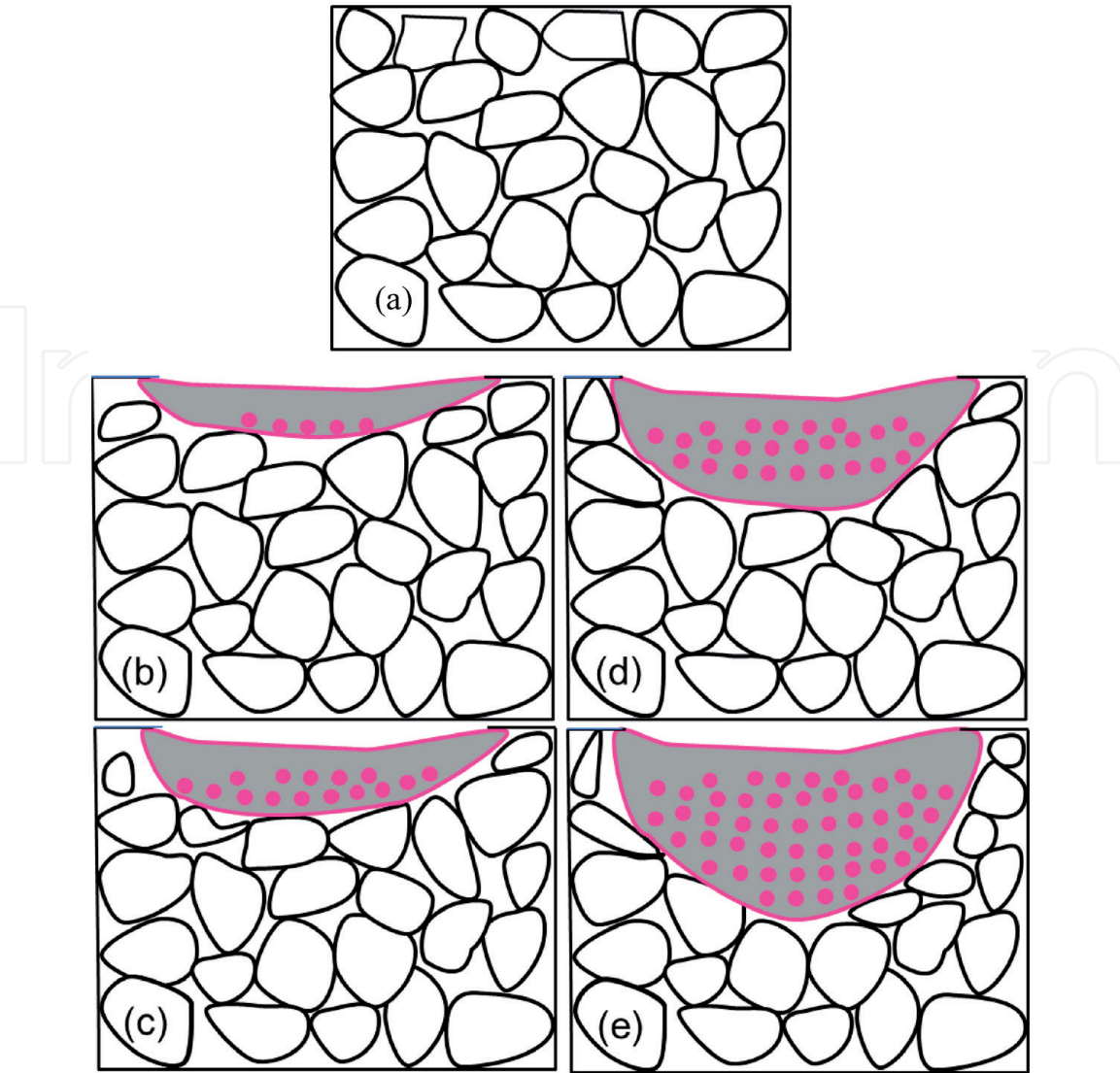


**Figure 9.** Schematic diagram of (a) As received AZ31B magnesium alloy, microstructure of laser fused layer of (b) laser melted at 1600 W, (c) laser melted at 1800 W, (d) laser melted at 2000 W.

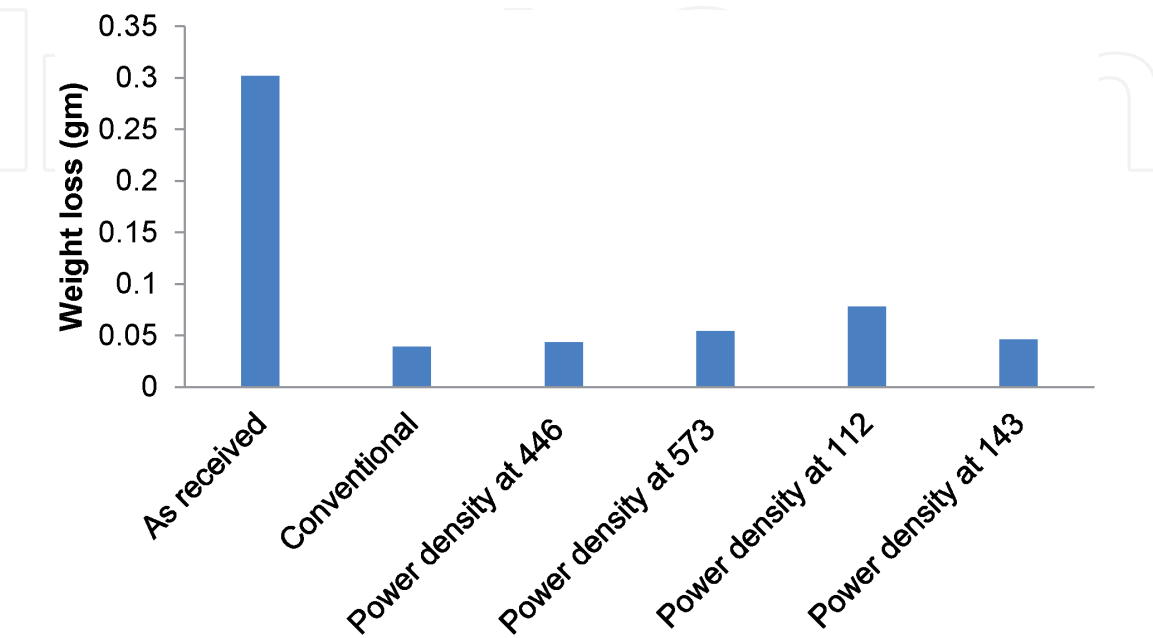


**Figure 10.** The effect different heat treatment on weight loss of AISI M2 tool steel.

due to the grain refinement, high dislocation density and dispersive distribution of  $\beta$ -Mg<sub>17</sub>Al<sub>12</sub> phase in the fused layer. [15].

The LSM method produced the higher surface roughness of AZ80 magnesium alloys compared to MB26 due to the variation in cooling rate. A nanosecond pulsed fiber laser with the wavelength of 1060 nm is used for the LSM process. The process parameters such as pulse duration, repetition rate, and spot size are 220 ns, 500 kHz, and 44  $\mu$ m, respectively. Alloys are irradiated with a laser power density of  $1.20 \times 10^7$  W/cm<sup>2</sup> and at a scanning speed of 200 mm/s with 50% beam bath overlapping. The higher microhardness was observed for MB26 than the AZ80 due to the higher melting layer thickness. [16]. The LSM is also used to study the grain size, microhardness of hybrid composites. The laser power is varied from 1.8 to 2.0 kW, the laser beam diameter range is 4.72–6.07 mm, standoff distance range is 35–45 mm and a constant scan speed of 400 mm/s is maintained. Argon shielding gas is used during the laser melting process to prevent the oxidation. The study found that the LSM treated hybrid metal matrix composite has lower grain size compared to untreated composites due to rapid solidification after LSM. The LSM produces the higher hardness of composites compared to untreated composite [17]. The effect of different laser power on microhardness and wear of AISI M2 high speed steel is studied by using LSM. The Nd: YAG laser, stand of distance varying from 1 to 2 cm, power varying from 600 to 1800 W, argon gas of 0.5 bar, laser spot varying from 2 to 4 mm and speed varying from 50 to 100 cm/min are used in this process. The results found that the maximum hardened depth of 0.85 mm is achieved by using power of 1400 W. The wear resistance of tool steel is nearly equal to conventionally hardened work material and it is shown in **Figure 10**. The reason for LSM produces high wear resistance and high hardened surface is due to the fine dendrites with dissolved carbides [18]. The LSM is also used to improve the hardness and wear resistance of Hastelloy C-276. The CW CO<sub>2</sub> laser with the parameters of 2 mm beam diameter, 0.6 MPa argon pressure, power varying from 1.25–1.75 kW, speed of 300 mm/min and interaction time of 400 ms are used in the work. The result found that the maximum hardness of 447 HV is achieved by using the power of 1.5 kW and scanning speed of 300 mm/min. The hardness is improved by 1.8 times compared to parent metal. The wear resistance of hastelloy is high in the sample laser treated at 1.5 kW of power and 300 mm/min speed and it is shown in **Figure 11**. This is due to the significant effect of grain refinement on hardness [19].

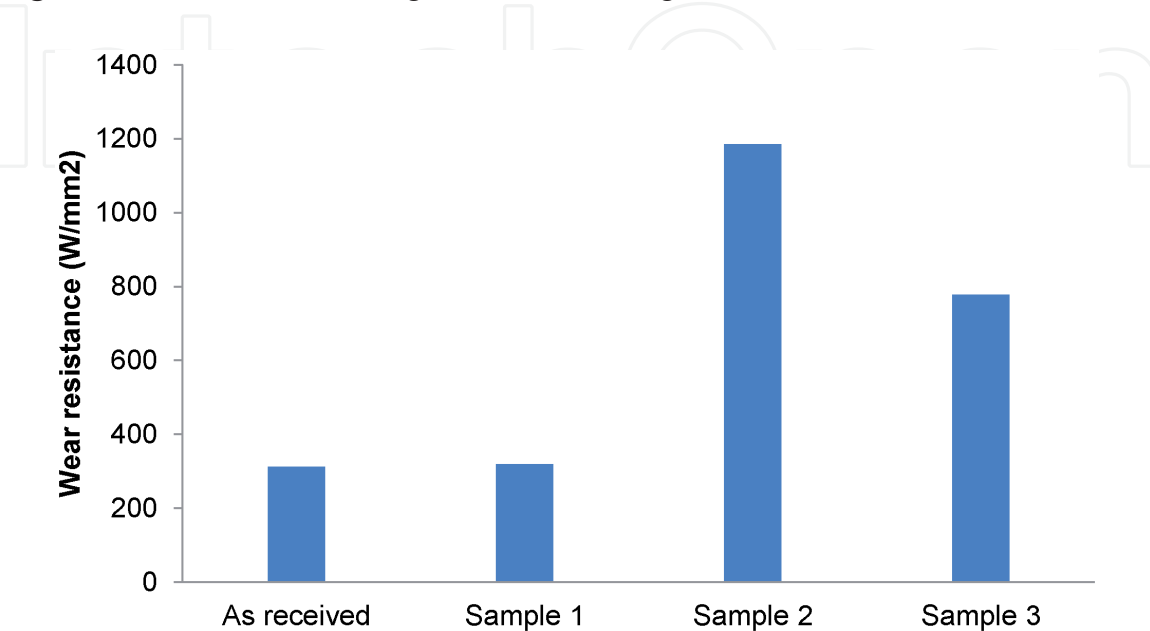


**Figure 11.**  
*The effect of LSM on wear resistance of Hastelloy C-276.*



The laser surface melting is carried out on nodular cast iron (NCI) [20]. The laser parameters, power of 1.5 kW, scan speed of 600 mm/min, overlapping of 30% and defocus of 15 mm and argon gas are used to melt the NCI surface. The microstructure of as received nodular cast iron showed with more ferrite and less pearlite as shown in **Figure 12a**. The  $\gamma$ -phase dendrites and an interdendritic carbide structure were observed in the laser treated region and it is shown in **Figure 12b**. The reason for forming dendrite in the laser treated region is due to the rapid heating and solidification. The needle shape interdendritic structure of  $\text{Fe}_3\text{C}$  and M-phase is also observed due to the higher cooling rate. The convection is also the reason for forming of homogeneous dendritic. The small diameter of nodules is also observed in the bottom layer with partial dissolution of nodular graphite due to the heat treatment and self-quenching. The uneven martensite and dendrite phases are observed in the intermediate layer due to the rapid re-solidification of the melt pool. Finally, fine martensite is observed in the bottom region. Moreover, no cracks and no voids are observed in the processed depth.

The worn out surface of as received and laser melted surface is shown in **Figure 13a** and **b**. The LSM specimen wear track showed with smooth, minor grooves and delamination. The wear depth and pile-up of laser processed specimens are lesser than untreated specimens. The laser treated surfaces have

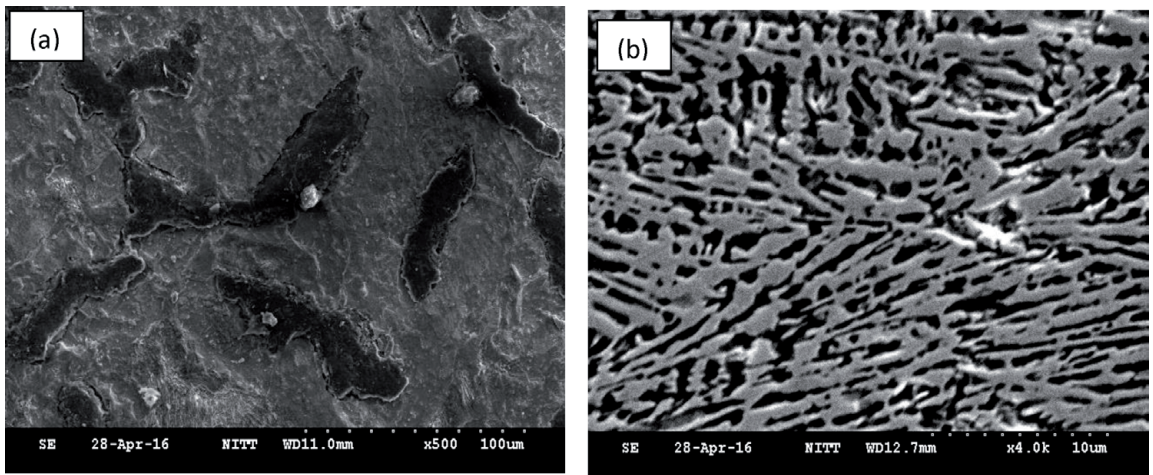


**Figure 12.**  
*Microstructure of; (a) as-received nodular cast iron, and (b) laser surface melted nodular cast iron.*

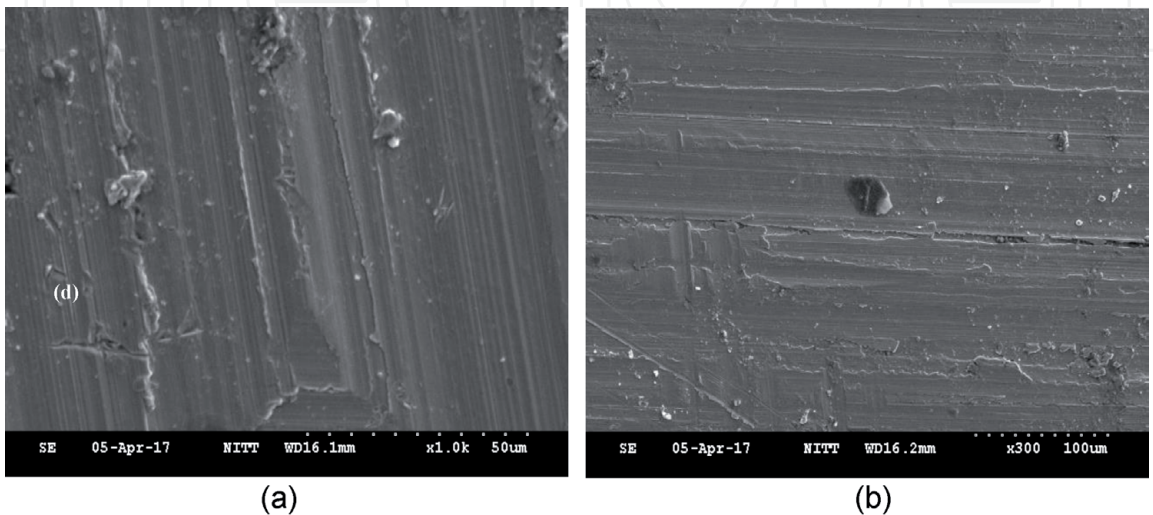


**Figure 13.**  
*Worn out surface of; (a) base metal, (b) laser melted specimen.*



fine grooves resulting in improving the wear resistance of specimens due to the microstructure changes. The root causes for improving the wear resistance of laser processed materials are fine M-phase and retained  $\gamma$ -phase with  $\text{Fe}_3\text{C}$  phase. The length of depth of hardness is increased by increasing the melted depth. The reasons are due to the precipitation hardening, residual stress by refinement of grains through rapid re-solidification. The cooling rate and thermal gradient also support the refinement of grains resulting in increased the hardness of the laser treated zone. Compared to hardness of substrate material, the laser processed depth has four time higher hardness due to the uniform grain structure. The partially melted zone shows the higher hardness due to the graphite nodules and fine ledeburite microstructure with the graphite interface. The wear loss is calculated for both the laser processed sample and untreated sample. The laser processed samples showed less wear than substrate.

#### 4. Laser surface alloying (LSA)

Laser surface alloying is a material processing technique that utilizes the focused laser sources and produces the high power density to melt the metal coating and a portion of the underlying substrate. The schematic view of laser surface alloying is shown in **Figure 14**. The schematic diagram of shape and dimensions of laser surface alloyed zone is shown in **Figure 15**. Here,  $W$  = width,  $T$  = thickness,  $B$  = build-up and  $D$  = melted depth. Aluminum alloys are widely used in automobile and aerospace applications due to the availability and low cost, ductility, good strength-to-weight ratio and lightweight. These alloys have low hardness and poor tribological properties which leads to wear problem. Hence, the additional protection is required to enhance the wear resistance properties to localized areas. So, LSA can be used to improve the surface properties of aluminum alloys, titanium alloys, magnesium alloys, copper alloys and nickel-copper alloys. The laser alloyed component properties are depending upon the selection of alloy material, composition and elemental surface distribution. These factors are affecting the microstructural

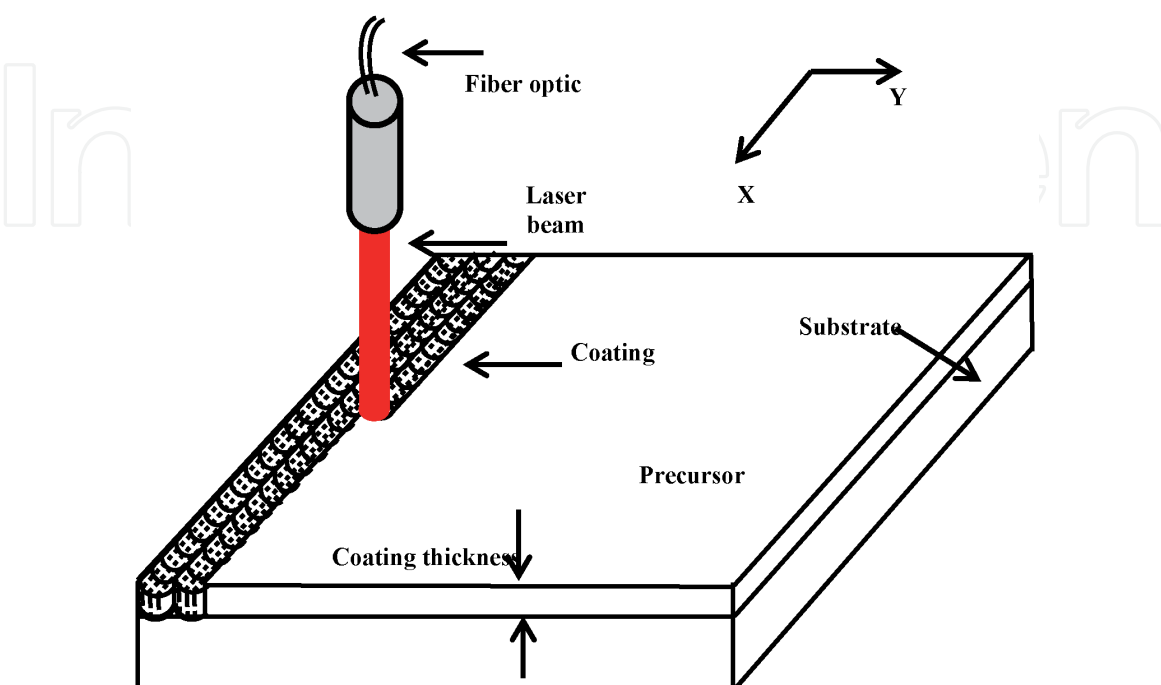


**Figure 14.**  
 Schematic view of laser surface alloying.

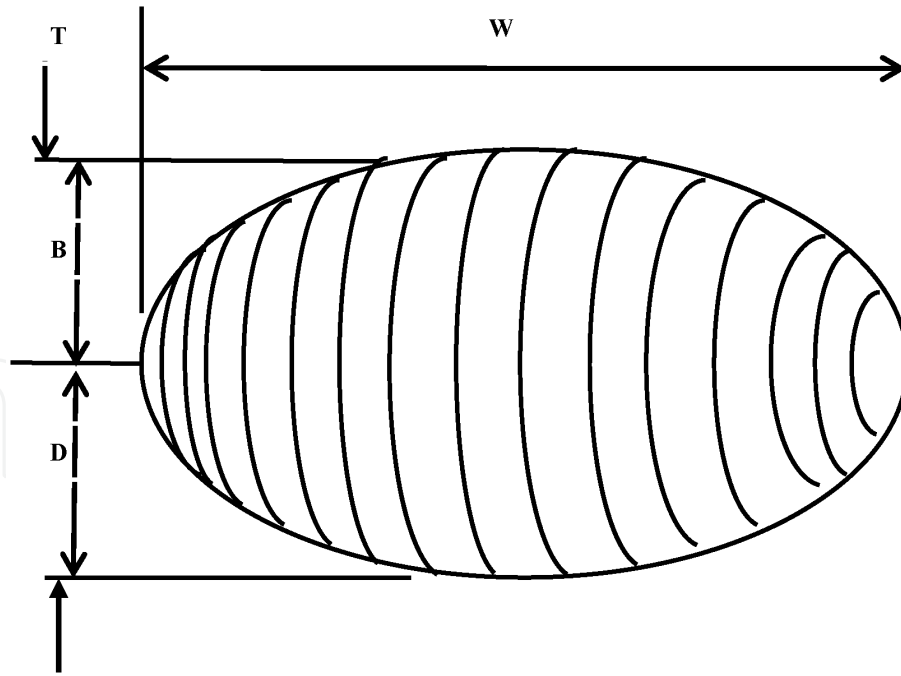


**Figure 15.**  
*Schematic diagram of shape and dimensions of laser surface alloyed zone.*

development in the alloyed surface. The ceramic alloys, carbide, oxide and boride ( $\text{SiC}$ ,  $\text{WC}$ ,  $\text{TiO}_2$ ,  $\text{TiB}_2$  and  $\text{TiC}$ ) are widely used as the coating material on aluminum alloys due to the low density, high hardness, good wear, high melting temperature and corrosion resistance. The hybrid ceramics, a component coating on aluminum produces better wear resistance than the single ceramics component coating. Titanium is added to the carbon resulting in forming  $\text{TiC}$  to improve the surface properties and by the same to prevent the formation of  $\text{Al}_4\text{C}_3$  carbides. A study on  $\text{FeCoCrAlCuNi}_x$  high entropy alloy coating on pure copper is carried out using LSA to evaluate the microhardness and wear. The laser power 1.7 kW, laser spot diameter 1.2 mm, scanning speed 2.0–3.0 mm/s, argon as shielding gas and flow rate 12 L/min are used in this process.

**Figure 16a** shows the microstructure of HEA  $\text{FeCoCrAlCuNi}_x$ . The HEA coating have high density, little holes and adequate metallurgical bonds to substrate. It is noticed that the dilution ratio of the tested HEA coating is higher than 20%. Typical dendrite and interdendrite structures are clearly observed in Ni05 and Ni10 HEAs (**Figure 16b** and **c**), while only one phase was observed for Ni15 HEA (**Figure 16d**). Compared to hardness of copper, coated copper produces higher hardness and it is shown in **Figure 17** [21]. The effect of addition of Ni–Cr–Si–B alloy to brass substrate was studied through LSA. The 2 kW CW Nd-YAG laser with a spot diameter of 3 mm, the laser power density varied between 141 and 212 W/mm, while the scanning speed is kept constant at 5 mm/s. Argon with a flow rate of 15 l/min is used as the shielding gas to prevent the oxidation. Laser surfacing is achieved by overlapping of adjacent tracks, with an overlapping ratio of 50%. The hardness of the modified layers increased slightly from the surface to a maximum and sharply fell to the value of the substrate at the interface between the treated layer and the substrate. The increases in hardness observed for the modified layer is attributed to the formation of hard borides [22]. The effects of addition of  $\text{SiC}$  and  $\text{TiO}_2$  to aluminum alloy are studied by continuous mode  $\text{CO}_2$  laser. The  $\text{CO}_2$  laser with the parameters of 1.7 kW, scan speed of 400 mm/min, standoff distance of 40 mm and laser beam diameter of 7.4 mm are used for  $\text{SiC}$  alloying. The  $\text{CO}_2$  laser with the parameters of 1.8 kW, scan speed of 300 mm/min, standoff distance of 30 mm and laser beam diameter of 5.8 mm are used for  $\text{TiO}_2$  alloying. The result found that the ceramic nature of  $\text{SiC}$

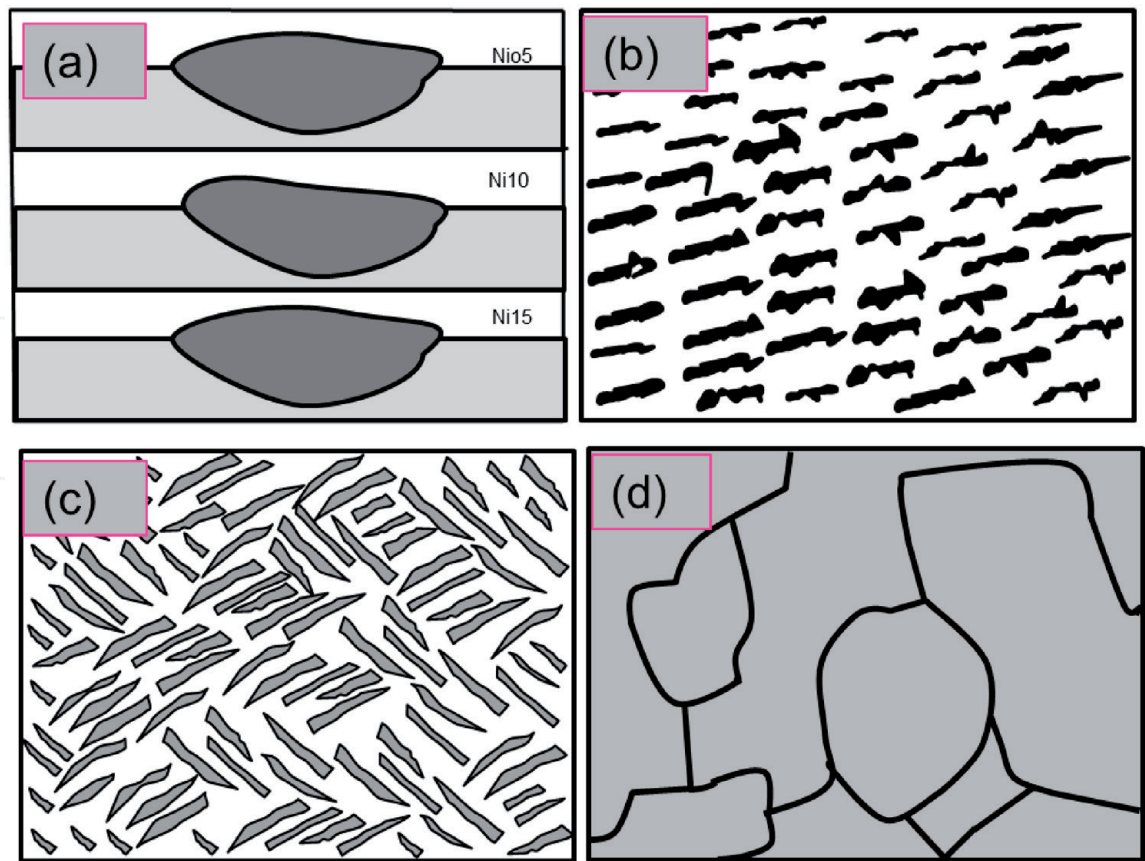


**Figure 16.**  
Microstructure images of (a) FeCoCrAlCuNi<sub>x</sub> HEA coatings on cross sectional view, (b) high magnifications image of Ni<sub>0.5</sub> HEA (c), Ni<sub>10</sub> HEA (d) and Ni<sub>15</sub> HEA.

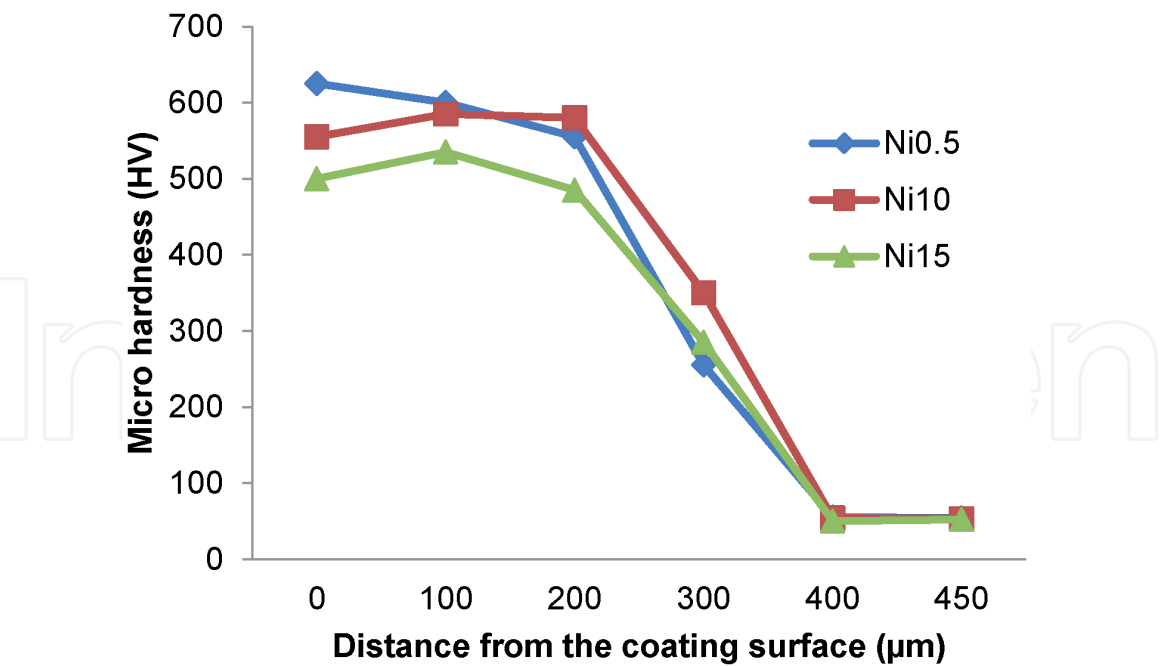


**Figure 17.**  
Microhardness of FeCoCrAlCuNi<sub>x</sub> HEA coatings.

and TiO<sub>2</sub> improved microhardness of alloyed zone from 30 HV<sub>0.3</sub> substrate material to 180 HV<sub>0.3</sub> with SiC and 220 HV<sub>0.3</sub> with TiO<sub>2</sub> [23].

A study on the effect of addition of WC + Co + NiCr to AISI 304 stainless steel through Nd: YAG laser. The 5 kW Nd: YAG with beam diameter of 4 mm, power varying from 1 to 3 kW, scan speed from 0.005–0.1 m/s and argon gas of 5 L/min are



used in the alloying process. The experimental result found that the LSA has been performed to form a defect free and uniform alloy zone. Compared to hardness of substrate, laser alloying produces the higher hardness due to the grain refinement [24].

The laser surface alloying is carried out on nodular cast iron by adding Ni-20%Cr alloy [20]. The laser parameters, power of 1.5 kW, scan speed of 600 mm/min, overlapping of 30% and defocus of 15 mm and argon gas are used to alloying the NCI surface. The microstructure of the laser alloyed specimen, worn out surface of substrate and laser alloyed specimen is shown in **Figure 18a–c** respectively. The ledeburite and pre-eutectic austenite are observed in the LSA surface. In addition,  $\gamma$ -phase (austenite) to M-phase (martensite) is transformation observed. The laser alloyed surface has produced the defect free and fine microstructure. The  $\gamma$ -phase has a higher percentage of Ni than cementite, whereas the Fe<sub>3</sub>C phase has Cr more and Ni less element. Hence, the presence of Fe<sub>3</sub>C on the laser-alloyed surface is rich in Cr and the  $\gamma$ -phase was supported through the solid solution of both alloy powders of Ni and Cr. The rapid solidification is the reason for obtaining the fine microstructure in the laser alloyed surface. The laser processed worn out surfaces have severe plastic deformation, wear track, delamination, grooves and adhesive particles. The NiCr alloying is also observed by using the LSA. The length of depth of hardness is increased by increasing the melted depth. The reasons are due to the refinement of grains through rapid re-solidification. The rate of cooling rate and thermal gradient also support the refinement of grains resulting in increased the hardness of the laser treated zone. Compared to hardness of substrate material, the laser processed depth has 2.62 time higher hardness due to the uniform grain structure. The wear loss is calculated for laser processed sample and untreated

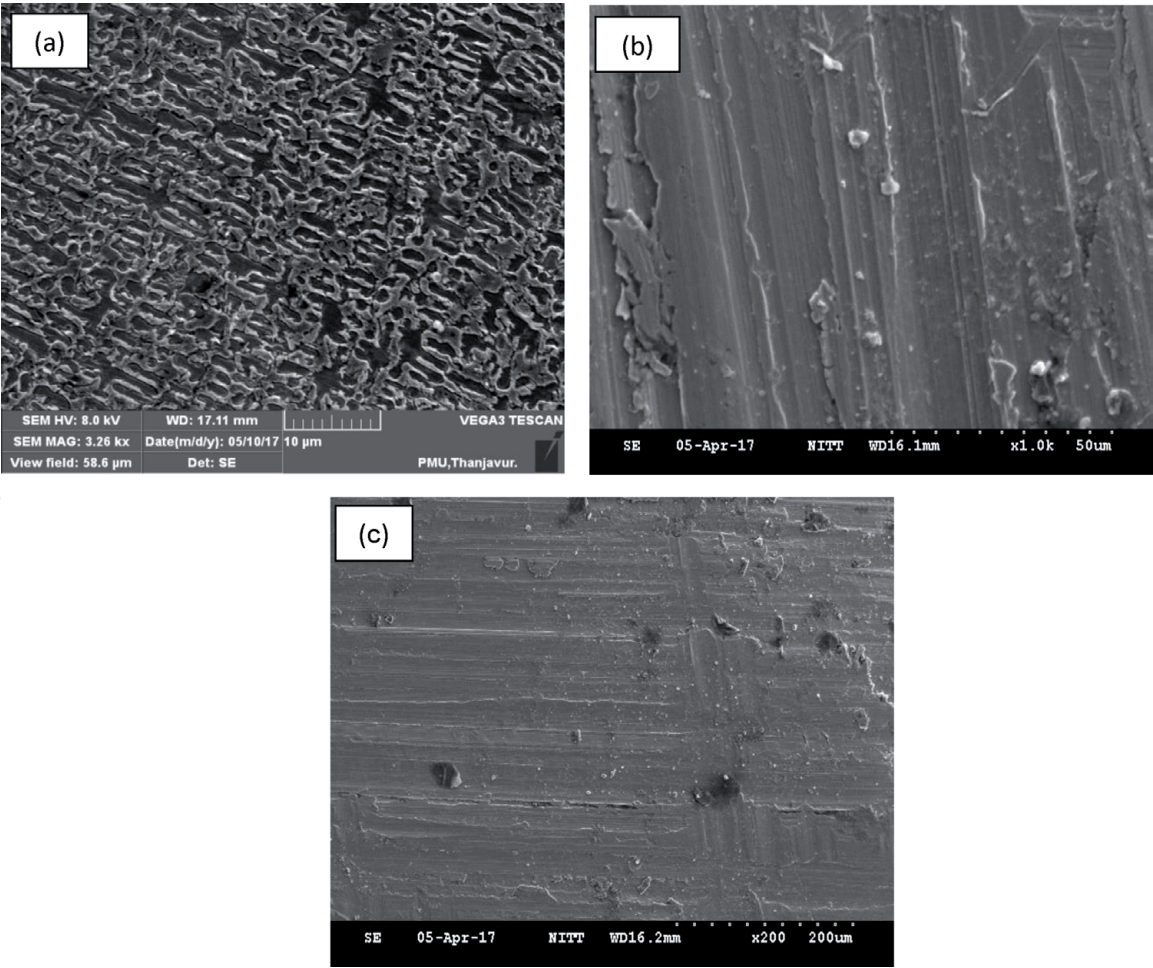


**Figure 18.** Microstructure of LSA specimen (a), worn out surface of substrate (b), and worn out substrate of LSA (c).

sample. The laser processed samples are produced lesser wear rate than substrate due to the improved hardness.

### 5. Laser cladding (LC)

Laser cladding is similar to arc welding. The laser is used to melt the clad material coated on the substrate. The powder, wire and strip form of clad materials are commercially available to perform by different laser processes. The major benefits of LC have low porosity, good surface uniformity and low dilution. The clad materials have rapid quench and cooling down after deposition resulted in a fine grained micro-structure. The laser is used to deposit clad material on substrate through the interaction of powder with laser. The substrate permits the melt pool to solidify and form the solid track. The schematic of laser cladding process is shown in **Figure 19**. Compared to other different surface processing used to enhance the wear and corrosion resistance of substrate, LC is an attractive alternative method. This is due to the intrinsic properties of laser radiation. The LC benefits are high input energy, low distortion, and minimum dilutions observed between the substrate, processing flexibility and cladding on small areas. The LC can be used in surface alloys and composites in order to achieve the required properties. The LC produces desired properties are obtained by varying the process parameters such as laser beam power density, laser beam diameter at the workpiece surface and laser beam travel speed.

The laser solution strengthening, laser surface alloying and laser cladding have highly correlation to corrosion and erosion resistance. The laser solution strengthening and laser surface alloying are used to improve the erosion and corrosion resistance of old components without changing their sizes whereas laser cladding is used to repair wasted components by restoring their size. The high entropy alloy of  $\text{CoCrFeNiNb}_x$  is coated to a pure titanium sheet by using laser cladding to study the hardness of the material. The laser cladding parameters such as power of 100 W, scanning speed of 8 mm/s, defocusing amount of +2 mm, pulse duration of 5 ms,

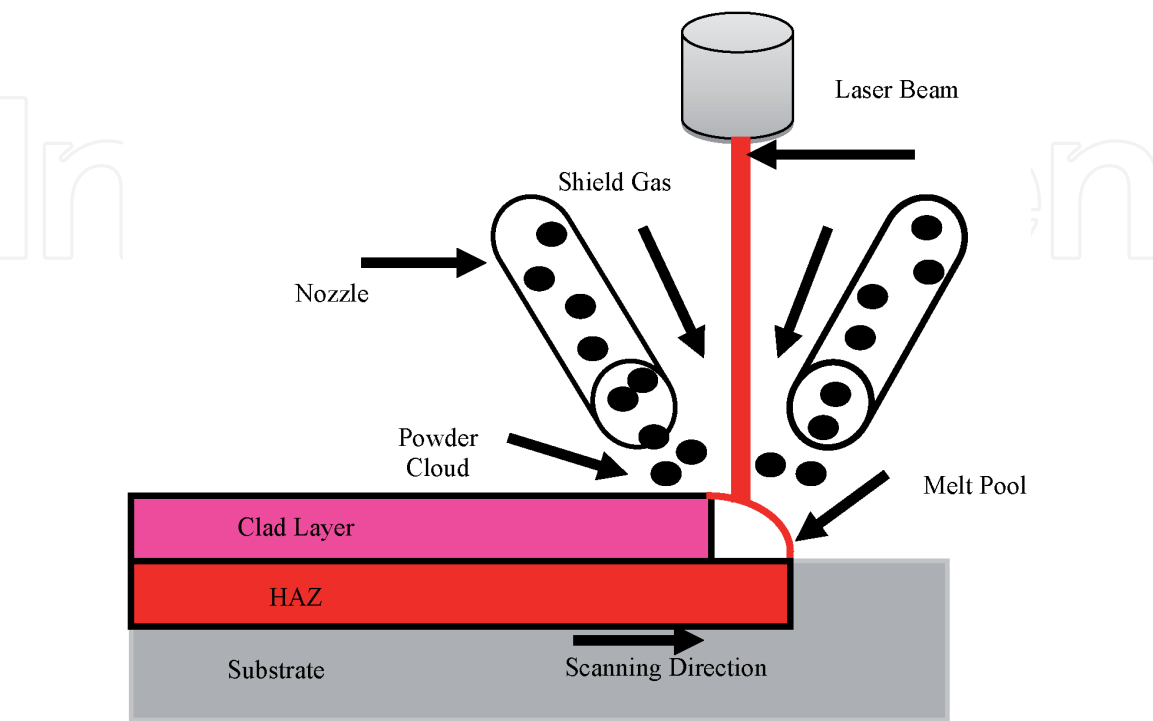


**Figure 19.**  
*Schematic of laser cladding process.*



frequency of 20 Hz, beam diameter of 1 mm power density of  $127.4 \text{ W/mm}^2$  and linear energy density of  $12.5 \text{ J/mm}$  are used in this process. The result found that the CoCrFeNiNb<sub>x</sub> HEA coated on titanium sheet produces higher hardness compared to the pure titanium. The Nb coating produces significant improvement in hardness compared to pure titanium due to the consisted phase of BCC solid solution with equiaxed bulk grain morphology and Cr<sub>2</sub>Ti Laves phase [25]. A comparison is performed between the thermal spray coating and laser cladding performance on steel. The laser cladding conditions, power of 780 W, cladding speed of 4.3 mm/s, powder feed rate of 6 g/min and argon gas are used. The thermal spray conditions, distance of 200 mm, acetylene (0.7 bar) and oxygen (4 bar) gas are used. The Metco 15E powder is used in both the processes. The result found that the cladded layer produced the high hardness, crack free, and good adherence to substrate whereas flame coating produces high porosity, minimum dilution and oxides inclusions [26]. The Inconel 625 coating performance on steel is evaluated by arc welding and laser cladding based on the microstructure, wear resistance and hardness. The parameters, power of 1200 W, scan speed of 2 mm/s, powder feed rate of 5 g/min, shielding gas flow rate of 5 L/min and powder feeding gas flow rate of 8 L/min are used. The result found that the arc welded and laser clad Inconel 625 coatings have Ni (fcc) solid solution phase, and fine microstructure. The arc welded coating to Inconel 625 is produced slightly lower hardness compared to laser cladding coating. This is due to the microstructure developed in the arc welding. The laser clad Inconel 625 coating is preferred due to its better mechanical performance such as hardness and wear resistance at both room and elevated temperature [27]. The 316 stainless steel powders coated on EN3 mild steel is to evaluate clad geometry and distribution of elements by laser cladding. The 2 kW continuous wave CO<sub>2</sub> with laser power 1.8 kW, beam spot diameter 2–5 mm, powder feed rate 0.160–0.220 g/s, substrate traverse speed 7–40 mm/s are used. The stainless steel powder coating provides the sound coating and no porosity [28]. The Fe-Cr-Si-B alloy powder coating is performed on low carbon steel using laser cladding to evaluate the microstructure, hardness, wear resistance and corrosion resistance. The result identified that the Fe-Cr-Si-B alloy powder coating provides higher wear resistance, high hardness and high corrosion resistance compared to substrate [29]. The CPM 15 V, CPM 10 V, CPM 9 V, D2 and M4 coatings are provided on AISI 1070 carbon steel by laser cladding. The laser cladding conditions, power varying from 2.5–2.75 W, laser beam diameter varying from 2 mm, substrate traverse speed varying from 7.6–8.6 mm/s, powder feed rate varying from 20 to 9 g/min and overlap varying from 30 to 50% are used in the process. The abrasive wear resistance of the laser-clad CPM 15 V and CPM 10 V coatings is superior performance than D2 steel, whereas the wear resistance of the CPM 9 V and M4 coatings is inferior to that of the D2 [30].

**Figure 20a** shows the microstructure of Colmonoy 6 cladding on Inconel 625 [31]. The laser cladding parameters are 400 mm/min speed, feed rate of 4 g/min, power of 1000 W, argon pressure of 1 bar with flow rate of 25 lpm and 150 degrees preheating used in this process. The clad surfaces have no defects, uniform dendrite eutectic phases observed. There are two regions represented in the clad surface such as darker region for boride content and lighter region for  $\gamma$ -nickel. The high quantity of intermetallic laves phase is observed in the clad surface. **Figure 20b** shows the worn out surface of substrate Inconel 625. Compared to wear intensity of sample, laser clad surfaces have lesser wear. The plow marks are also observed in the worn out surface substrate due to the less wear resistance and high plastic deformation. The higher material removal rate of the sample is observed than the clad surface. **Figure 20c** shows the laser clad worn out surface. The few debris particles, few depth of wear track and few grooves are observed in the clad surface. This is due to the high hardness of the clad layer. Therefore, better

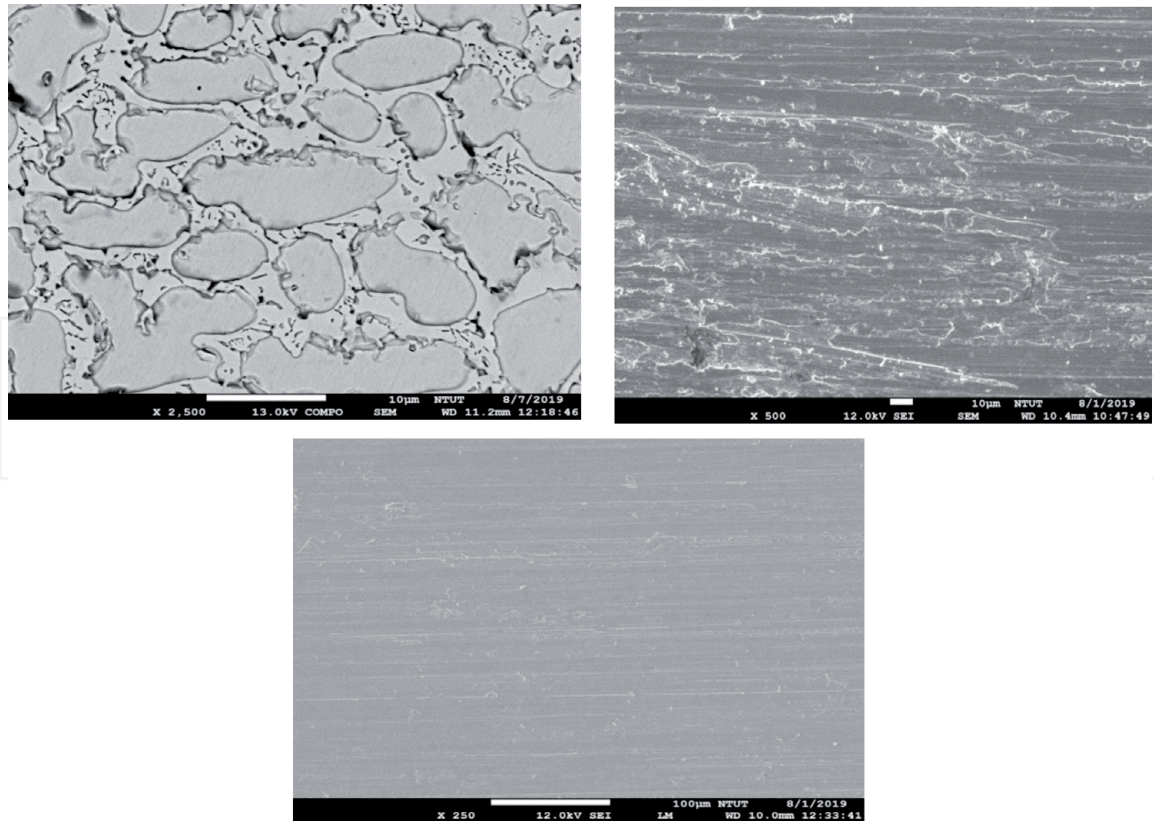


**Figure 20.**  
 Microstructure of Colmonoy 6 clad (a), worn out surface of substrate (b) and worn out surface of laser cladding (c).

protection is provided by the clad layer over the untreated surface. The more hardness is observed in the clad surface than the base metal. The reasons for increasing the hardness of clad surface is due to the defect free cladding, proper fusion and laves phase presented. The reason for decreasing the hardness of base material is due to weak intermetallic phases.

The coefficient of friction (CoF) and wear behavior of coated and substrate found that the CoF is increased with increased sliding distance due to the reduced adhesion resistance and increasing heat between points of contact. The more CoF is observed in the substrate sample than clad sample due to the adhesion effect. The less CoF is observed in the clad sample due to the hard laves phases. It is found that low mass loss is observed in the clad sample compared to base material. The wear loss is highly related to the hardness and base material produces poor wear resistance when compared to clad surface.

## 6. Laser texturing

Laser texturing is a process that alters a material surface property by modifying its texture and roughness. The laser beam creates micro patterns on the surface through laser ablation, removing layers with micrometer precision and perfect repeatability. Typical patterns include dimples, grooves, and free forms. Laser surface texturing can be used to improve properties like adherence, wettability, electrical and thermal conductivity, and friction. For example, the method can increase surface adherence before applying common coatings like adhesives, paint or ceramic. Laser texturing can also be used to prepare surfaces for thermal spray coating and laser cladding as well as to improve the performance of mechanical seals. Surface treatments like abrasive blasting and chemical etching processes need

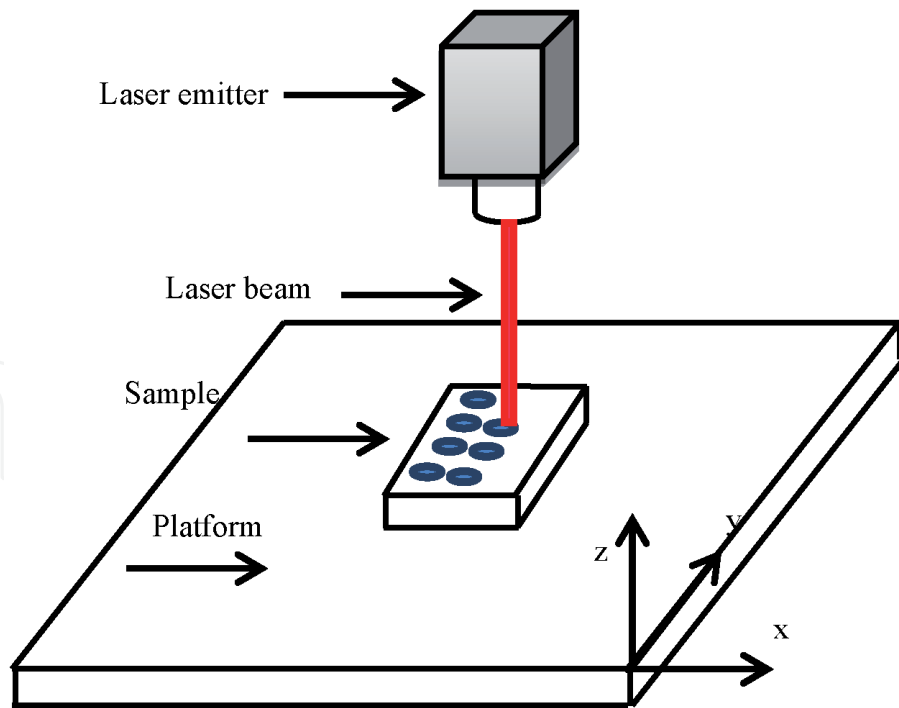


**Figure 21.**  
*Schematic of laser texturing process.*

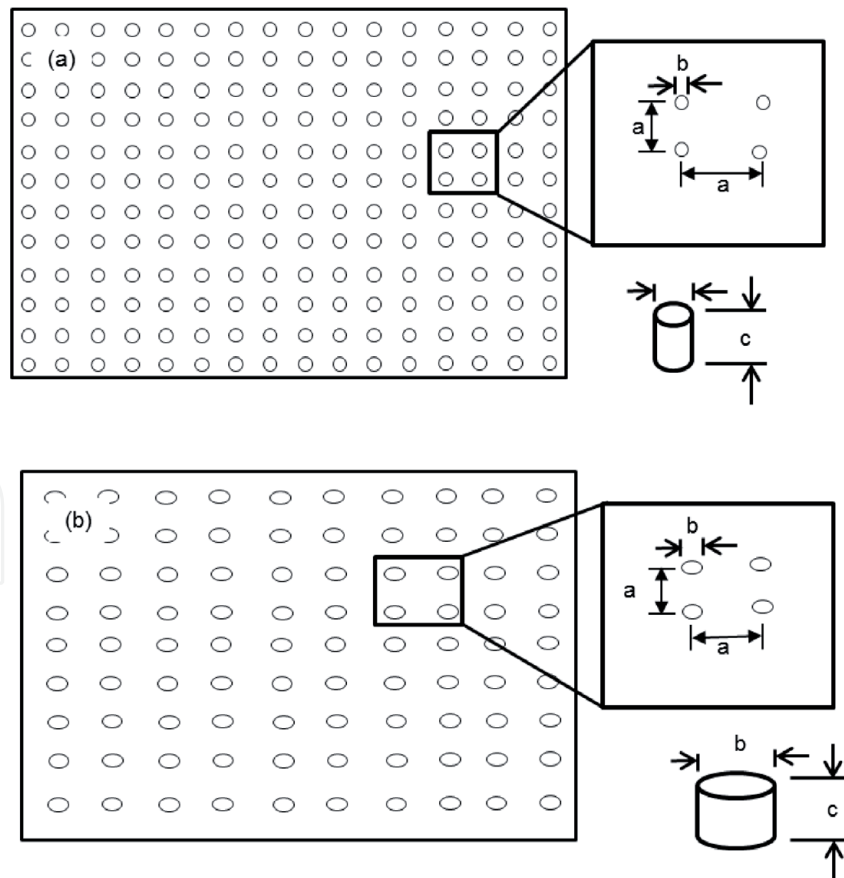


**Figure 22.**  
*Schematic of laser surface texture dimensions: (a) circle, (b) oval.*

consumables like steel grits and acid to texture surfaces. Unlike those treatments, the laser texturing process functions without consumables. This results in low operating costs, low maintenance, and improved health and safety in the workplace.

Operators will not need to handle chemicals, wear protective equipment, and stop operations to replace consumables. Laser texturing uses laser ablation to selectively remove materials from specific surface areas. By adjusting the laser's parameters, the surface is removed as well as creates different patterns. This typically increases roughness, creating surface textures that can easily lodge adhesives and provide additional anchoring surface. To reach the material's ablation threshold, pulsed lasers concentrate energy to reach a high peak power. Typically, the pulse duration is 100 nanoseconds, and each pulse contains between 0.5 and 1 millijoules. The time required to texture a surface depends on the material, the desired roughness level, and the laser system's output power. The application of laser texturing is in adhesive bonding, mechanical seals, painting and coatings. The laser texturing process is shown in **Figure 21**. The circle and oval shape dimple texturing on metal can be made using a laser and the schematic diagram is shown in **Figure 22 a-b**. Where,  $a$  = pitch,  $b$  = diameter, and  $c$  = height.

## 7. Conclusion

The new materials have been developed every day to meet the demand of competitive situations. The surface properties of substrate can be improved by a number of methods such as laser surface alterations such as surface hardening, melting, alloying, cladding and texturing in order to improve the mechanical performance and tribological behavior. In this work, the effect of laser process parameters on microstructure, hardness and wear rate of materials have been presented. The laser surface hardening is needed to high stressed components namely gear teeth, gears, shafts, camshafts, axles, cylinder liners and exhaust valves. The laser surface melting can be adopted in biomedical alloys, sport cars and power plants made of stainless steel, magnesium alloy and superalloys. The locomotive, aerospace and structural components made of aluminum alloys, titanium alloys and magnesium alloys have required the laser surface alloying to improve the surface properties of metals. The repaired and refurbishment components such as internal combustion engine parts, gas turbine, turbine blades and tools are highly needed the laser surface cladding to improve the surface properties of metals. The texturing on material is used to increase the tribological characteristics of materials resulting in improved surface roughness, wettability, improve load capacity, wear rates, lubricating lifetime and reduce friction coefficient. Hence, the laser based surface modification techniques can be adopted to improve the performance of the components.

## Acknowledgements

The authors wish to thank the Ministry of Science and Technology, Taiwan ROC for the financial support to carry out this work.

## Conflict of interest

The authors declare that they have no conflicts of interest in the work.



IntechOpen

## Author details

Natarajan Jeyapraakash<sup>1\*</sup>, Che-Hua Yang<sup>1,2</sup> and Durairaj Raj Kumar<sup>3</sup>

1 Additive Manufacturing Center for Mass Customization Production, National Taipei University of Technology, Taipei-10608, Taiwan, ROC

2 Institute of Manufacturing Technology, National Taipei University of Technology, Taipei-10608, Taiwan, ROC

3 Department of Mechanical Engineering, MAM School of Engineering, Tiruchirappalli-621 105, India

\*Address all correspondence to: prakash84gct@gmail.com; prakash@ntut.edu.tw

## IntechOpen

© 2020 The Author(s). Licensee IntechOpen. This chapter is distributed under the terms of the Creative Commons Attribution License (<http://creativecommons.org/licenses/by/3.0>), which permits unrestricted use, distribution, and reproduction in any medium, provided the original work is properly cited. 



## References

- [1] Totten, G.E. (2006) *Steel Heat Treatment: Equipment and Process Design Handbook*, 2nd ed., Taylor and Francis Group.
- [2] Tani, G., Orazi, L. and Fortunato, A. (2008) 'Prediction of hypo eutectoid steel softening due to tempering phenomena in laser surface hardening', *CIRP Annals-Manufacturing Technology*, Vol. 57, pp.209-212.
- [3] Carrera-Espinoza, R., Rojo Valerio, A., del Prado Villasana, J., Yescas Hernández, J.A., Moreno-Garibaldi, P., Cruz-Gómez, M.A. and Figueroa López, U. (2020) 'Surface Laser Quenching as an Alternative Method for Conventional Quenching and Tempering Treatment of 1538 MV Steel', *Advances in Materials Science and Engineering*.
- [4] Liu, Q., Song, Y., Yang, Y., Xu, G. and Zhao, Z. (1998) 'On the laser quenching of the groove of the piston head in large diesel engines', *Journal of materials engineering and performance*, Vol. 7, pp.402-406.
- [5] Wang, B., Pan, Y., Liu, Y., Lyu, N., Barber, G.C., Wang, R., Cui, W., Qiu, F. and Hu, M. (2020) 'Effects of quench-tempering and laser hardening treatment on wear resistance of gray cast iron', *Journal of Materials Research and Technology*, Vol. 9, pp. 8163-8171.
- [6] Slatter, T., Taylor, H., Lewis, R. and King, P. (2009) 'The influence of laser hardening on wear in the valve and valve seat contact', *Wear*, Vol. 267, pp.797-806.
- [7] Pashby, I.R., Barnes, S. and Bryden, B.G. (2003) 'Surface hardening of steel using a high power diode laser', *Journal of Materials Processing Technology*, Vol. 139, pp.585-588.
- [8] SeDao, Hua, M., Shao, T.M. and Tam, H.Y. (2009) 'Surface modification of DF-2 tool steel under the scan of a YAG laser in continuously moving mode', *Journal of Materials Processing Technology*, Vol. 209, pp.4689-4697.
- [9] Rana, J., Goswami, G.L., Jha, S.K. Mishra, P.K. and Prasad, B.V.S.S.S. (2007) 'Experimental studies on the microstructure and hardness of laser-treated steel specimens', *Optics and Laser Technology*, Vol. 39, pp.385-393.
- [10] Barka, N., Sattarpanah Karganroudi, S., Fakir, R., Thibeault, P. and Feujofack Kemda, V.B., 2020. Effects of Laser Hardening Process Parameters on Hardness Profile of 4340 Steel Spline—An Experimental Approach. *Coatings*, 10(4), p.342.
- [11] Zhou, W., Zhou, Y., Wu, N. and Maharjan, N., 2019. Laser surface hardening of AISI 1055 steel in water submerged condition.
- [12] Zhou, J., Xu, J., Huang, S., Hu, Z., Meng, X. and Feng, X., 2017. Effect of laser surface melting with alternating magnetic field on wear and corrosion resistance of magnesium alloy. *Surface and Coatings Technology*, 309, pp.212-219.
- [13] Majumdar, J.D., Galun, R., Mordike, B.L. and Manna, I., 2003. Effect of laser surface melting on corrosion and wear resistance of a commercial magnesium alloy. *Materials Science and Engineering: A*, 361(1-2), pp.119-129.
- [14] Zhang, L., Yu, G., Li, S., He, X., Xie, X., Xia, C., Ning, W. and Zheng, C., 2019. The effect of laser surface melting on grain refinement of phase separated Cu-Cr alloy. *Optics & Laser Technology*, 119, p.105577.
- [15] Cui, Y., 2018. Influence of laser surface melting on tribological behaviour of AZ31B. *Surface Engineering*, 34(4), pp.296-300.

- [16] Li, Y., Arthanari, S. and Guan, Y., 2019. Influence of laser surface melting on the properties of MB26 and AZ80 magnesium alloys. *Surface and Coatings Technology*, 378, p.124964.
- [17] Bannaravuri, P.K., Birru, A.K. and Dixit, U.S., 2020. Effect of laser surface melting on surface integrity of Al– 4.5 Cu composites reinforced with SiC and MoS<sub>2</sub>. *Transactions of Nonferrous Metals Society of China*, 30(2), pp.344-362.
- [18] Newishy, M., Abdel-Aleem, H., Elkousy, M.R., El-Mahallawi, I. and El-Batahgy, A., 2018. Surface Treatment of AISI M2 Tool Steel by Laser Melting. In *Key Engineering Materials* (Vol. 786, pp. 128-133). Trans Tech Publications Ltd.
- [19] Hashim, M. and Duraiselvam, M., 2015. Enhancing tribological and corrosion resistance of Hastelloy C-276 through laser surface treatment. In *Materials Science Forum* (Vol. 830, pp. 659-662). Trans Tech Publications Ltd.
- [20] Jeyapragash, N., Yang, C.H., Duraiselvam, M. and Sivasankaran, S., 2020. Comparative study of laser melting and pre-placed Ni–20% Cr alloying over nodular iron surface. *Archives of Civil and Mechanical Engineering*, 20(1), pp.1-12.
- [21] Wu, C.L., Zhang, S., Zhang, C.H., Zhang, H. and Dong, S.Y., 2017. Phase evolution and properties in laser surface alloying of FeCoCrAlCuNi high-entropy alloy on copper substrate. *Surface and Coatings Technology*, 315, pp.368-376.
- [22] Tam, K.F., Cheng, F.T. and Man, H.C., 2002. Enhancement of cavitation erosion and corrosion resistance of brass by laser surface alloying with Ni–Cr–Si–B. *Surface and Coatings Technology*, 149(1), pp.36-44.
- [23] Jiru, W.G., Sankar, M.R. and Dixit, U.S., 2017. Investigation of microstructure and microhardness in laser surface alloyed aluminium with TiO<sub>2</sub> and SiC powders. *Materials Today: Proceedings*, 4(2), pp.717-724.
- [24] Chakraborty, A., Pityana, S.L. and Dutta Majumdar, J., 2017. Laser surface alloying of AISI 304 stainless steel with WC+ Co+ NiCr for improving wear resistance, *Procedia Manufacturing*, 7, pp. 8-14.
- [25] Xiang, K., Chen, L.Y., Chai, L., Guo, N. and Wang, H., 2020. Microstructural characteristics and properties of CoCrFeNiNb<sub>x</sub> high-entropy alloy coatings on pure titanium substrate by pulsed laser cladding. *Applied Surface Science*, p.146214.
- [26] Pascu, A., Hulka, I., Tierean, M.H., Croitoru, C., Stanciu, E.M. and Roată, I.C., 2016. A comparison of flame coating and laser cladding using Ni based powders. In *Solid State Phenomena* (Vol. 254, pp. 77-82). Trans Tech Publications Ltd.
- [27] Feng, K., Chen, Y., Deng, P., Li, Y., Zhao, H., Lu, F., Li, R., Huang, J. and Li, Z., 2017. Improved high-temperature hardness and wear resistance of Inconel 625 coatings fabricated by laser cladding. *Journal of Materials Processing Technology*, 243, pp.82-91.
- [28] Weerasinghe, V.M., Steen, W.M. and West, D.R.F., 1987. Laser deposited austenitic stainless steel clad layers. *Surface engineering*, 3(2), pp.147-153.
- [29] Yang, Yan CJ and Wang 1987 Laser cladding of FeCrSiB alloy *Lasers* 14 548-52
- [30] Wang, S.H., Chen, J.Y. and Xue, L., 2006. A study of the abrasive wear behaviour of laser-clad tool steel coatings. *Surface and Coatings Technology*, 200(11), pp.3446-3458.

[31] Jeyaprakash, N., Yang, C.H. and Ramkumar, K.R., 2020. Microstructure and wear resistance of laser cladded Inconel 625 and Colmonoy 6 depositions on Inconel 625 substrate. *Applied Physics A*, 126, pp.1-11.

IntechOpen

IntechOpen